

Preparation of High-Quality a-Si:H using Cluster-Suppressed Plasma CVD Method and Its Prospects

Yukio Watanabe, Masaharu Shiratani, Kazunori Koga

Department of Electronics, Kyushu University, Hakozaki 6-10-1 Fukuoka 812-8581, Japan

Fax: 81-92-642-3973, e-mail: watanabe@ed.kyushu-u.ac.jp

Si-particles in a range below 10nm in size (referred to as clusters) exist in SiH₄ high-frequency discharges, and their density amounts to 10¹¹cm⁻³ even under conditions for which device-quality a-Si:H films are deposited. The study on growth kinetics of such clusters has made much progress. On the other hand, it has been pointed out that a-Si:H films with a low SiH₂ bond density C_{SiH_2} show less light-induced degradation and C_{SiH_2} increases with the density of higher-order-silane (HOS) radicals [Si_nH_x (n<5, x< 2n+2)]. However, HOS radicals usually coexist with clusters. Hence, our group has developed cluster-suppressed plasma CVD reactors aiming at identifying which of HOS radicals and clusters is more responsible for formation of the SiH₂ bonds and also at realizing a-Si:H films of little light-induced degradation. The studies show the following: C_{SiH_2} linearly increases with a volume fraction V_f of clusters incorporated into films, while the HOS density correlate little with C_{SiH_2} ; For Schottky solar cells of our films, initial and stabilized fill factors are much higher and the degradation ratio is much smaller than those of conventional films respectively. Such studies suggest that high-rate-deposition of a-Si:H films of little light-induced-degradation will be realized by further developing this cluster-suppressing plasma CVD method.

Key words: a-Si:H, SiH₂, cluster, higher-order-silane, plasma CVD

1. INTRODUCTION

Suppression of light-induced degradation of hydrogenated amorphous silicon (a-Si:H) films has been an important issue for a-Si:H solar cells [1,2]. A-Si:H films with a low Si-H₂ bond density C_{SiH_2} have been found to show less light-induced degradation (or high stability) [3], while the mechanism leading to their correlation has not been revealed yet. This suggests that the C_{SiH_2} should be reduced to obtain higher stability of the films, and also species responsible for the SiH₂ bond formation should be identified. There coexist higher-order silane (HOS) Si_mH_n ($m < 4$, $n \leq 2m+2$) in a size range below about 0.5 nm and particles in a size range of about 0.5-10 nm (clusters) in SiH₄ discharges [4-11]. The HOSs and clusters have possible to be incorporated into the films during the deposition. Concerning the SiH₂ bond formation, Matsuda and co-workers have proposed the contribution of HOS related radicals [3,12]. On the other hand, we have recently proposed that the clusters are mainly responsible for its formation. In order to obtain the detailed information of clusters, we have already developed photon-counting laser-light scattering (PCLLS) and downstream-cluster-collection (DCC) method realizing their highly sensitive detection [13]. Information of the HOSs can be obtained with quadrupole mass spectrometer (QMS) [14]. In order to identify which of HOSs and clusters mainly contribute to the SiH₂ information, we have to carry out such measurements using the same reactor as and under the

same experimental conditions as those for the film deposition experiments.

In this paper, we report such experimental results, and based on the results we identify the important species responsible for the SiH₂ bond formation in a-Si:H films. Moreover, we report some results of Schottky cells of a-Si:H films.

2. EXPERIMENTAL

Experiments were carried out using a capacitively-coupled high-frequency discharge reactor of a diode or triode configuration as shown in Fig. 1. The diode configuration was employed both for detecting clusters by the DCC method and HOSs such as Si₂H₆ and Si₃H₈ by QMS and also for depositing a-Si:H films. The triode configuration was employed only for the film deposition [13, 15, 16]. The reactor is of the cluster-suppressed plasma CVD type; the growth of clusters is suppressed by utilizing gas viscous and thermophoretic forces exerted on clusters together with reducing the stagnation regions of gas flow. For the triode configuration, the flux of clusters to the substrate was reduced by cutting off them with the grounded electrode mesh as well as by utilizing that the clusters diffuse slowly as compared to SiH₃ radicals, being predominant deposition species. Powered and grounded electrodes for the diode and the triode was placed 18 mm and 15 mm apart, respectively, in a

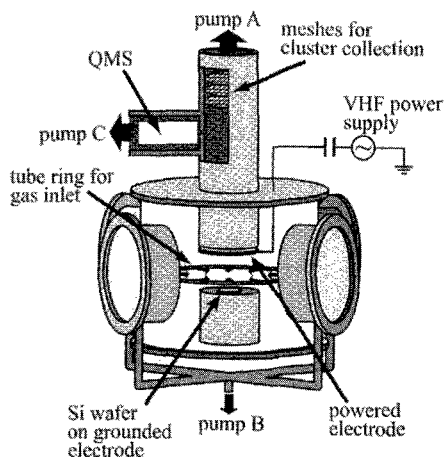


Fig. 1. Cluster-suppressed plasma CVD reactor of diode configuration.

stainless steel vessel of 315 mm in diameter and 250 mm in height. All the electrode were made of stainless steel and their diameter was 120 mm. Gas of SiH_4 was supplied towards the center axis of the discharge column through 44 holes of 1 mm in diameter bored in a tube ring, as shown in Fig. 1, of 240 mm in diameter, which was placed at 10 mm above the grounded electrode for the diode. The flow rate and pressure were 30 sccm and 9.3 Pa, respectively. The excitation frequency and supplied power density were 60 MHz and 0.015-0.15 W/cm^3 , respectively. The reactor was pumped out through both the powered electrode and four ports on the side wall of the reactor by two molecular drag pumps (pumps A and B in Fig. 1). The gas flow through the powered electrode caused by the pump A reduces cluster growth in the radical generation region around the plasma/sheath boundary. When the substrate is heated up to 250 °C, the gas temperature gradient drives clusters above a few nm in size toward the powered electrode of room temperature [4]. The pump B was employed to reduce accumulation of clusters in the reactor due to the stagnation of gas flow.

To measure the density of SiH_4 , $[\text{SiH}_4]$, as well as those of H_2 , $[\text{H}_2]$, Si_2H_6 , $[\text{Si}_2\text{H}_6]$, and Si_3H_8 , $[\text{Si}_3\text{H}_8]$, in the discharges, the gas passed through the powered electrodes was sampled through an orifice of 2 μm in diameter to analyze with a QMS (ANELVA M-QA100TS) as shown in Fig. 1. Size and density of clusters were measured by the ex-situ DCC and in-situ PCLLS methods [7, 13]. For the DCC method, clusters were trapped on three stainless steel meshes placed parallel in series in the pumping port connected to the powered electrode as shown in Fig. 1. The efficiency of

cluster trapping by the three meshes was estimated to be above 95 % [17]. Information on size distribution, density, shape and structure of the trapped clusters were obtained with a high-resolution transmission electron microscope (TEM: JEOL 2010). For the PCLLS method, size of clusters was deduced from their coagulation rate after turning off the discharge and, using their size value, their density was done from the absolute light intensity [7].

For deposition experiments, a-Si:H films of 1 μm in thickness were prepared on two kinds of Si wafers at a substrate temperature of 250 °C. The one is Si (111) wafers with a high resistivity (1000- 5000 Ωcm) for the measurements of C_{SiH_2} , and the other is $n^+\text{Si}$ (100) wafers for the measurements of fill factors (FF) of a $n^+\text{Si}/\text{a-Si:H}/\text{Ni}$ Schottky solar cells. For the C_{SiH_2} measurements, an absorption intensity profile in a range of 1750- 2350 cm^{-1} of spectrum measured with a Fourier-transform infrared (FTIR) spectroscope (JASCO FT/IR-620) was deconvoluted into two profiles: a peak of the one profile is at 2090 cm^{-1} , and a peak of the other is at 2000 cm^{-1} . The C_{SiH_2} value was deduced from the intensity value at 2090 cm^{-1} [18]. For the FF measurements, FF was evaluated irradiating the Schottky cell by an AM 1.5 solar spectrum light of 100 mW/cm^2 (1 SUN) at $T_s = 30$ °C. The stabilized FF was measured after 7.5 hours light soaking under conditions of 2.4 SUN (240 mW/cm^2) irradiation and $T_s = 60$ °C.

3. RESULTS AND DISCUSSION

3.1 Overview of growth kinetics of clusters

We will briefly review initial growth processes of clusters in low-pressure and low-power pure SiH_4 RF discharges. Figure 3 shows the typical time evolution of size and density of small clusters (corresponding to HOS), large clusters, and particles. The sizes of large clusters for $t=0.2$ and 0.9 s are 2.3 and 9.3 nm, respectively. These clusters grow in size at the growth rate of 10 nm/s, which significantly exceeds the film deposition rate of 0.1 nm/s on the grounded electrode. The density of large clusters is $1.5 \times 10^{11} \text{ cm}^{-3}$ for $t=0.2$ s and it decreases to $1.1 \times 10^{10} \text{ cm}^{-3}$ for $t=0.9$ s. The density for $T_{\text{on}}=0.2-0.9$ s is more than one order of magnitude higher than the positive-ion density measured with a Langmuir probe, indicating that a large proportion of the particles below 10 nm in size are neutral.

3.1 Rate equations of SiH_3 and Si_nH_x

To obtain information on an effective parameter for suppressing the cluster growth, we have

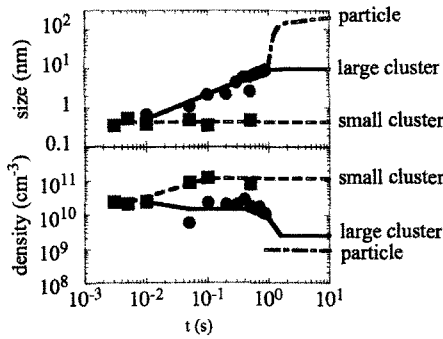


Fig. 2. Typical time evolution of size and density of small clusters, large clusters, and particles. SiH₄(100%), 13 Pa.

identified the dominant loss process for SiH₃, being the predominant film precursor, and Si_nH_x information using rate equations of their densities. The rate equation of the SiH₃ density [SiH₃] may be given by

$$\frac{d[\text{SiH}_3]}{dt} = k_d n_e [\text{SiH}_4] - k_r [\text{SiH}_3]^2 - \frac{D_1}{\Lambda_1^2} [\text{SiH}_3] - \frac{[\text{SiH}_3]}{\tau_{res}}$$

where [SiH₄] is the SiH₄ density, n_e the electron density, k_d the rate coefficient for SiH₃ generation due to electron impact dissociation of SiH₄, k_r the rate coefficient of self recombination of SiH₃ in gas phase, D₁ the diffusion coefficient of SiH₃, Λ₁ the diffusion length, τ_{res} the gas residence time in the discharge space. As the diffusion loss term is dominant for SiH₃ radicals under the conditions in this study, their steady state density is mainly determined by the balance between the diffusion loss term, being the third term in the right hand side (RHS) of the equation and the generation term, being the first term in RHS.

The rate equation of the density of higher order silane and clusters [Si_nH_x] may be given by

$$\frac{d[\text{Si}_n\text{H}_x]}{dt} = k_n [\text{SiH}_2][\text{Si}_{n-1}\text{H}_{x-2}] - k_{n+1} [\text{SiH}_2][\text{Si}_n\text{H}_x] - \frac{D_n}{\Lambda_n^2} [\text{Si}_n\text{H}_x] - \frac{[\text{Si}_n\text{H}_x]}{\tau_{res}}$$

where k_n, k_{n+1} the rate coefficients for the gas phase reaction between SiH₂ and Si_{n-1}H_{x-2}, Si_nH_x, respectively, D_n the diffusion coefficient of Si_nH_x. For heavy or stable Si_nH_x species, the loss due to gas flow surpasses the diffusion loss term, their steady state density is mainly determined by the balance between the gas flow loss term, being the third term in the right hand side (RHS) of the equation and the generation term, being the first term in RHS.

The steady state densities of SiH₃ and Si_nH_x have

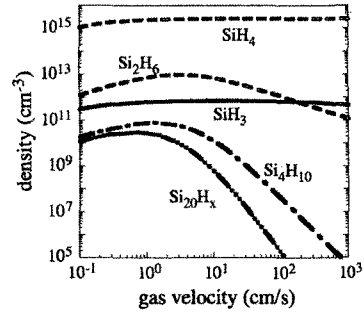


Fig. 3. Dependence of SiH₃ and Si_nH_x densities on gas velocity. Electrode distance 2 cm, SiH₄ (100%), 13 Pa. Absolute densities at a gas velocity of 3 cm/s are calibrated using experimental values obtained by QMASS and double pulse discharge methods.

been calculated for one dimensional gas flow reactor. The results are shown in Fig. 3. Under the conventional gas velocity around a few cm/s, the Si_nH_x densities are close to their maximum values., The densities decrease considerably with increasing the gas velocity from 1 cm/s to 100 cm/s, while the SiH₃ density remains nearly constant. The higher density decrease is obtained

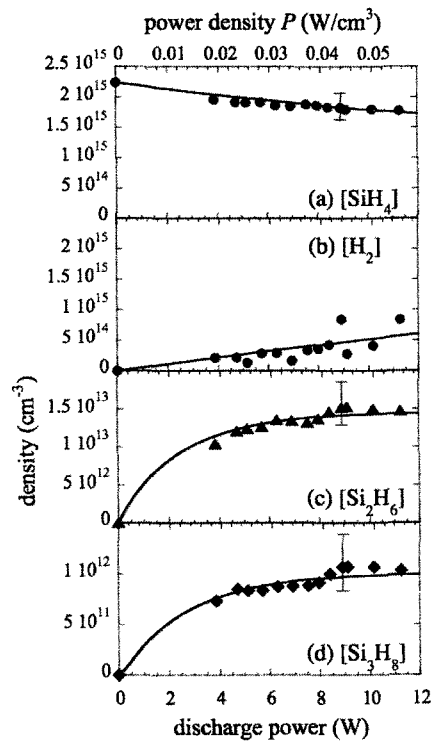


Fig. 4. Discharge power dependence of densities of (a)SiH₄, (b)H₂, (c)Si₂H₆ and (d)Si₃H₈ in steady state during discharge. Discharge conditions: SiH₄ 100%, 30 sccm, 9.3 Pa, 60 MHz, T_s=250°C.

for Si_nH_x of the larger n . Therefore, a high gas velocity above 10 cm/s is effective in reducing the Si_nH_x densities, especially for the large n value.

3.2 Higher-order silane

To obtain information on contribution of HOS radicals such as Si_2H_5 and Si_3H_7 to the film growth compared to that of SiH_3 , being the predominant deposition radical, we have carried out QMS measurements to deduce SiH_4 , Si_2H_6 , and Si_3H_8 densities, since SiH_3 , Si_2H_5 and Si_3H_7 radicals are mainly generated from SiH_4 , Si_2H_6 , and Si_3H_8 , respectively, due to electron impact dissociation in the discharges. The densities of these molecules have been deduced from the intensities using a calibration procedure described in [12]. Figure 4 shows the discharge power dependence of the densities. The density of SiH_4 , $[\text{SiH}_4]$, decreases with increasing the discharge power, indicating the enhancement of dissociation of SiH_4 with an increase in the discharge power. The density of H_2 molecules linearly increases with the discharge power, as they are the main by-product due to the dissociation of SiH_4 . Both the densities of $[\text{Si}_2\text{H}_6]$ and $[\text{Si}_3\text{H}_8]$ increase with the discharge power. The power dependence in Fig. 4 can be explained by a simple reaction model[19].

We have estimated the contribution of HOS radicals to the film growth using the assumption as follows. The rate equation of the steady state density of $\text{Si}_m\text{H}_{2m+1}$ ($m=1, 2$ and 3) radicals may be given by

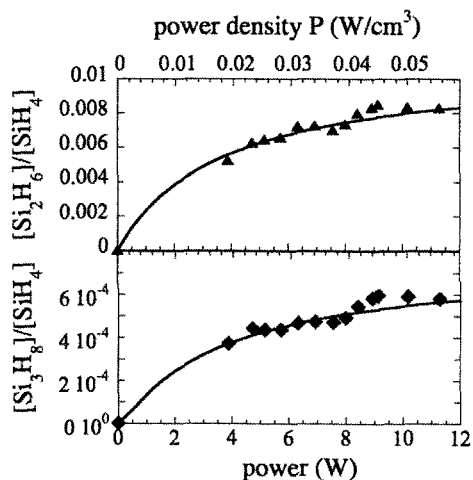


Fig. 5. Discharge power dependence of densities of (a) $[\text{Si}_2\text{H}_6]/[\text{SiH}_4]$ and (b) $[\text{Si}_3\text{H}_8]/[\text{SiH}_4]$ in steady state during discharge. Discharge conditions: SiH_4 100%, 30 sccm, 9.3 Pa, 60 MHz, $T_s=250^\circ\text{C}$.

$$\frac{d[\text{Si}_m\text{H}_{2m+1}]}{dt} = k_{dm}n_e[\text{Si}_m\text{H}_{2m+2}] - \frac{[\text{Si}_m\text{H}_{2m+1}]}{\tau_m},$$

where k_{dm} is the rate coefficient of $\text{Si}_m\text{H}_{2m+1}$ generation due to electron impact dissociation of $\text{Si}_m\text{H}_{2m+2}$ and τ_m the characteristic lifetime of $\text{Si}_m\text{H}_{2m+1}$. The steady state density of $\text{Si}_m\text{H}_{2m+1}$ can be written in the form

$$[\text{Si}_m\text{H}_{2m+1}] = \tau_m k_{dm} n_e [\text{Si}_m\text{H}_{2m+2}].$$

Since SiH_3 is the main film growth precursor in SiH_4 discharges, the contribution ratio of HOS radicals to the films growth is given by

$$\frac{[\text{Si}_m\text{H}_{2m+1}]}{[\text{SiH}_3]} \propto \frac{[\text{Si}_m\text{H}_{2m+2}]}{[\text{SiH}_4]} \quad (m=2 \text{ and } 3).$$

Figure 5 shows power dependence of $[\text{Si}_2\text{H}_6]/[\text{SiH}_4]$ and $[\text{Si}_3\text{H}_8]/[\text{SiH}_4]$. Both the ratios increase in a sub-linear way.

3.3 Clusters

To discuss the contribution of clusters to formation of SiH_2 bonds in films, we have measured dependence of the volume fraction V_f on discharge power. The results are shown in Fig. 6. While the data points in the figure are rather scattered, the V_f value increases in a super-linear way with the discharge power. This power dependence is quite different from those of $[\text{Si}_2\text{H}_6]/[\text{SiH}_4]$ and $[\text{Si}_3\text{H}_8]/[\text{SiH}_4]$ in Fig. 5.

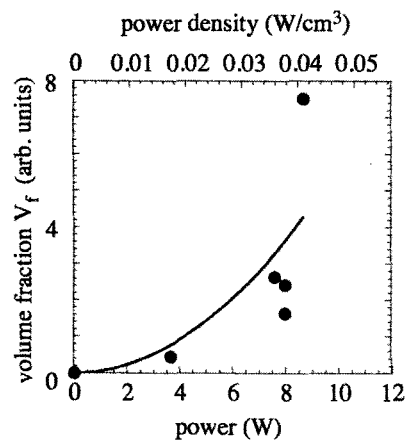


Fig. 6. Discharge power dependence of densities of volume fraction of clusters incorporated into films. Discharge conditions: SiH_4 100%, 30 sccm, 9.3 Pa, 60 MHz, $T_s=250^\circ\text{C}$.

3.4 SiH_2 content in a-Si:H films

In order to examine whether the HOS radicals contribute to formation of Si-H_2 bonds in a-Si:H films or not, dependence of C_{SiH_2} on the discharge power has been obtained under the same

conditions as those in Fig. 5. The results are shown in Fig. 7. The C_{SiH_2} value increases in a super-linear way with the discharge power, in other words, the C_{SiH_2} value varies in a way quite similar to that of V_f . This tendency indicates that the incorporation of clusters above about 1nm in size into a-Si:H films is an important origin of the Si-H₂ bond formation of interest. The lack of correlation between the ratios $[Si_2H_6]/[SiH_4]$, $[Si_3H_8]/[SiH_4]$ and the C_{SiH_2} value strongly suggests that the HOS radicals *do not* mainly contribute to formation of SiH₂ bonds in a-Si:H films.

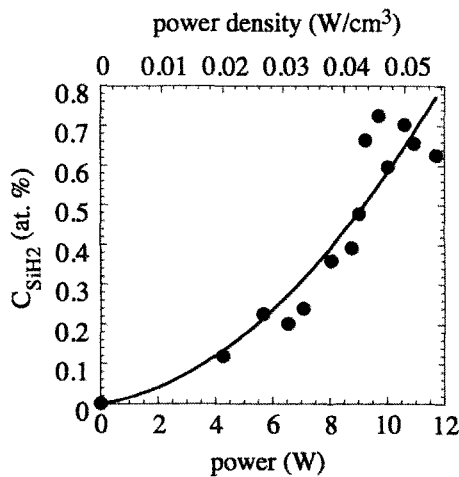


Fig. 7. Discharge power dependence of densities of SiH₂ bond density C_{SiH_2} in films. Discharge conditions: SiH₄ 100%, 30 sccm, 9.3 Pa, 60 MHz, Ts=250°C.

3.5 Fill factor of Schottky cells

The results described in sections 3.1-3.4 indicate that the quality of a-Si:H can be improved reducing V_f . Thus, we have employed the cluster-suppressed plasma CVD reactor of the triode configuration instead of the diode one. As the transmittance of the mesh used is 65 % and the

sticking probability of clusters and surface reaction probability of SiH₃ radicals are considered to be about 1 and 0.3, respectively, the V_f value and deposition rate of SiH₃ for the triode configuration are estimated to be reduced by about 75 % and 19 % compared to those for the diode, respectively. The light-induced degradation of film qualities has been evaluated preparing the Schottky solar cell. Table I shows the results for the cluster-suppressed triode together with those for the cluster-suppressed and conventional diode plasma CVDs; The initial and stabilized FF values of Schottky cell for the triode are 0.60 and 0.56, respectively. This degradation ratio is 6.7%, being quite low compared to the ratios of 12.5 and 17.0% for the cluster-suppressed and conventional diodes, respectively. A stabilized FF of 0.56 is equal to an initial FF for the cluster-suppressed diode and exceeds an initial FF of 0.53 for the conventional diode.

4. CONCLUSIONS

We have developed cluster-suppressed plasma CVD reactors aiming at identifying which of HOS radicals and clusters is more responsible for formation of the SiH₂ bonds and also at realizing a-Si:H films of little light-induced degradation. The studies show the following: The C_{SiH_2} value linearly increases with the volume fraction V_f of clusters incorporated into films, while the HOS density correlates little with C_{SiH_2} ; For Schottky solar cells of our films, initial and stabilized fill factors are much higher and the degradation ratio is much smaller than those of conventional films. Such studies suggest that high-rate-deposition of a-Si:H films of little light-induced-degradation will be realized by further developing this cluster-suppressing plasma CVD method.

5. ACKNOWLEDGEMENTS

This work was partly supported by a Grant-in-Aid for Scientific Research (A) from the Japan Society of the Promotion of Science (KAKENHI 14205047) and the New Energy and Industrial Technology Development Organization (NEDO). We wish to express our sincere thanks to Dr. A.

Table I. Initial and stabilized FF values and degradation ratios for films deposited using cluster-suppressed triode and diode plasma CVDs together with those for films deposited using conventional diode plasma CVD.

deposition method	initial FF	stabilized FF	degradation rate	conditions
cluster-suppressed triode plasma CVD	0.60	0.56	6.7 %	SiH ₄ 100%, 30sccm, 9.3Pa, 60MHz, 4W, Ts= 250°C, transmittance of the triode mesh: 64.5%
	0.60	0.56	6.7 %	SiH ₄ 100%, 30sccm, 9.3Pa, 60MHz, 4W, Ts= 250°C, transmittance of the triode mesh: 49.3%
cluster-suppressed diode plasma CVD	0.56	0.49	12.5 %	SiH ₄ 100%, 30sccm, 9.3Pa, 80MHz, 8W, Ts= 250°C
	0.56	0.48	14.3 %	SiH ₄ 100%, 30sccm, 9.3Pa, 80MHz, 8W, Ts= 280°C
conventional diode plasma CVD	0.52-0.48	0.47-0.36	9.6-25.0 %	SiH ₄ 100%, Ts= 250°C, [20]
	0.53	0.44	17.0 %	SiH ₄ 100%, 30sccm, 9.3Pa, 80MHz, 8W, Ts= 200°C

Matsuda and M. Kondo, AIST, for providing QMS. We also wish thank Messrs T. Kinoshita and H. Matsuzaki who contributed greatly to the preparation of the experimental setup. The FTIR measurements were carried out at the Center of Advanced Instrumental Analysis, Kyushu University.

Kondo, and A. Matsuda, *Thin Solid Films* **345** (1999) 75.

(Received December 23, 2004; Accepted January 31, 2005)

6. REFERENCES

- [1] D. L. Staebler, C. R. Wronski, *Appl. Phys. Lett.* **31** (1976) 292.
- [2] R. E. I. Schropp, M. Zeman, *Amorphous and Microcrystalline Silicon Solar Cells*, Kluwer Academic Publishers, Boston, 1998, p. 47.
- [3] T. Nishimoto, M. Takai, H. Miyahara, M. Kondo, A. Matsuda, *J. Non-Crys. Solids.* **299** (2002) 1116.
- [4] M. Shiratani, S. Maeda, K. Koga, Y. Watanabe, *Jpn. J. Appl. Phys.* **39** (2000) 287.
- [5] K. Koga, Y. Matsuoka, K. Tanaka, M. Shiratani, Y. Watanabe, *Appl. Phys. Lett.* **77** (2000) 196.
- [6] K. Koga, M. Shiratani, and Y. Watanabe, *Proceedings of the Nano-Technology Workshop, Korea, 2002*, p. 13.
- [7] M. Shiratani, Y. Watanabe, *Rev. of Laser Eng.* **26** (1998) 449.
- [8] M. Shiratani, T. Fukuzawa, Y. Watanabe, *Jpn. J. Appl. Phys.* **38** (1999) 4525.
- [9] Y. Watanabe, M. Shiratani, T. Fukuzawa, K. Koga, *J. Tech. Phys.* **41** (2000) 505.
- [10] M. Shiratani, T. Fukuzawa, K. Eto, Y. Watanabe, *Jpn. J. Appl. Phys.* **31** (1992) L1791.
- [11] Y. Watanabe, M. Shiratani, K. Koga, *Plasma Sources & Sci. Technol.* **11** (2002) A229.
- [12] M. Takai, T. Nishimoto, T. Takagi, M. Kondo, A. Matsuda, *J. Non-Cryst. Solids* **266** (2000) 90.
- [13] K. Koga, N. Kaguchi, M. Shiratani, Y. Watanabe, *J. Vac. Sci. & Technol. A* **22** (2004).
- [14] J. Perrin, O. Leroy, M.C. Bordage, *Contrib. Plasma Phys.* **36** (1996) 3.
- [15] Y. Watanabe, A. Harikai, K. Koga, M. Shiratani, *Pure Appl. Chem.* **74** (2002) 483.
- [16] K. Koga, M. Kai, M. Shiratani, Y. Watanabe, N. Shikatani, *Jpn. J. Appl. Phys.* **41** (2002) L168.
- [17] K. Koga, T. Kakeya, M. Shiratani, Y. Watanabe (unpublished).
- [18] M. H. Brodsky, M. Cardona, J. J. Cuomo, *Phys. Rev. B* **16** (1977) 3556.
- [19] K. Koga, N. Kaguchi, M. Shiratani, and Y. Watanabe, *Proc. MAPEES* (2004) in press.
- [20] T. Takagi, R. Hayashi, G. Ganguly, M.